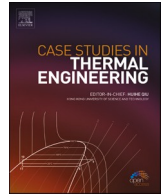




ELSEVIER

Contents lists available at ScienceDirect

Case Studies in Thermal Engineering

journal homepage: www.elsevier.com/locate/csite

A computational case study on the thermal performance of a rectangular microchannel having circular pin-fins

Mahdi Tabatabaei Malazi^{a,*}, Kenan Kaya^a, Ahmet Selim Dalkılıç^{b,*}

^a Department of Mechanical Engineering, Faculty of Engineering, Istanbul Aydın University, Istanbul, 34295, Türkiye

^b Department of Mechanical Engineering, Faculty of Mechanical Engineering, Yıldız Technical University, Istanbul, 34349, Türkiye

ARTICLE INFO

Handling Editor: Huihe Qiu

Keywords:

Microchannel

Pin-fin

Nusselt number

Pressure drop

Apparent friction factor

ABSTRACT

This paper concerns the hydraulic and thermal performances of a three-dimensional rectangular microchannel with circular pin-fins. Laminar flow with Reynolds values (Re) between 50 and 150 was investigated. A total of 20 cases were considered. Fifteen of them were carried out for circular pin-fins with 3 fin spacing-to-fin diameter ratios ($l/d = 2, 4, \text{ and } 6$) and 5 Re values ($Re = 50, 75, 100, 125, \text{ and } 150$) for a constant fin height-to-channel height ratio ($h/H = 0.25$). The others were run without the use of circular pin-fins in the computational domain. The pressure drop and velocity distribution contour plots were obtained. Average outlet temperature and average Nusselt number (Nu) were used to study microchannels' thermal performances. The validation process was performed for the Nu and friction factor, with absolute errors of less than 2% and 7%, respectively. The increase in Re and decrease in fin spacing caused an increase in Nu and a decrease in average outlet temperature. The pressure drop increased with increasing Re and number of fins. Therefore, thermal and hydraulic performances were found to depend on them. The predicted results indicated that the maximum average outlet temperature, pressure drop, and Nu were obtained for the smallest l/d . Comparing the microchannel with $l/d = 2$ to the microchannel without fins for $Re = 150$, the average outlet temperature of the microchannel with $l/d = 2$ is increased by nearly 0.23%. At Re of 150, the pressure decrease in the microchannel with $l/d = 2$ is nearly 23% greater than in the microchannel without fins. The average Nu of the microchannel with $l/d = 2$ is approximately 9% greater than that of the microchannel without fins when the Re is 150.

Nomenclature

A	cross-sectional area, m^2
c_p	specific heat capacity, J/kgK
d	fin diameter, μm
D_h	hydraulic diameter, m
f_{app}	apparent friction factor
k	thermal conductivity, W/mK
L	length, μm

* Corresponding author.

** Corresponding author.

E-mail addresses: mahditabatabaei@aydin.edu.tr (M. Tabatabaei Malazi), dalkilic@yildiz.edu.tr (A.S. Dalkılıç).

<https://doi.org/10.1016/j.csite.2023.103111>

Received 6 February 2023; Received in revised form 15 May 2023; Accepted 20 May 2023

Available online 8 June 2023

2214-157X/© 2023 The Authors. Published by Elsevier Ltd. This is an open access article under the CC BY-NC-ND license (<http://creativecommons.org/licenses/by-nc-nd/4.0/>).

l	fin spacing, μm
H	channel height, μm
h	fin height, μm
h_{ave}	average heat transfer coefficient, $\text{W}/\text{m}^2\text{K}$
HT	heat transfer
HTC	heat transfer coefficient
Nu	Nusselt number
Nu_x	local Nussult number
MC	microchannel
p	pressure, Pa
PD	pressure drop
Re	Reynolds number
T_i	average inlet temperature, K
T_o	average outlet temperature, K
T_w	bottom wall temperature, K
T_b	bulk fluid temperature, K
q	heat flux, kW/m^2
U_{in}	uniform inlet velocity, m/s
u	velocity component, m/s
\vec{u}	velocity vector
VG	vortex generator
W	width, μm
x, y and z	coordinates
<i>Greek symbols</i>	
ρ	density, kg/m^3
μ	dynamic viscosity, kg/ms
τ_w	wall shear stress, Pa
ΔP	pressure drop, Pa
ε	absolute errors, %

1. Introduction

Devices such as computers and electronic chips play an important role in engineering. They are expected to work in certain conditions to obtain optimum performance. Excess heat can destroy them. As a result of a rise in the pressure placed on the reliability and performance of systems as well as the shrinking of devices, thermal consideration has emerged as a critical component in the design of electronic packaging at all levels, from the chip level to the system level. Regarding this problem, microchannels (MCs) are one of the qualified solutions to control the heat in microelectronic devices and improve their efficiency.

Many devices that use a single-phase liquid flow use MCs. Micromachine components such as micropumps, microvalves, and microsensors were used in the first applications. Naturally, the advancements in microelectromechanical devices call for similarly compact heat removal systems. In the absence of any modifications to the transport processes or the emergence of any novel physical phenomena, it is anticipated that the laminar flow-friction factor and the heat transfer (HT) equations developed from theoretical considerations will remain true in MC applications. High relative roughness levels are more often seen in MCs, which have been considered a way of solving HT problems. MCs are utilized in numerous applications because of their dimensional characteristics and high efficiency. Hydraulic parameters, such as the hydraulic diameter of the MC, and the fins' height and diameter can affect MC performance, or in other words, HT rate and pressure drop (PD), directly. The recent numerical investigations, including those of passive HT enhancement techniques on the MCs, heat sinks, and MCs with nanofluid flows, are summarized in the following paragraphs.

Lee et al. [1] conducted experiments to study the HT and flow characteristics in the various rectangular MCs. The findings were attained for MC widths and Re ranging from 194 to 534 μm and 300 to 3500, respectively. The MC was made of copper, and they used water as a coolant fluid in their experimental setup. They showed that the heat transfer coefficient (HTC) depended on the channel size. The HTC increased when the channel size decreased. After some experimental studies, they estimated the MC HT rate following a numerical method.

Lu et al. [2] investigated three MCs with various wall surface roughness values in laminar flow numerically. The researchers applied square, wavy, and dimpled channel types. Their operating conditions included a fixed Re of 50 and a heat flux of 0.5 W/mm^2 from the bottom. The results showed that not only the modifications in wall surface roughness but also the PD increased the HT rate and Nu in the MC.

Dey and Saha [3] researched the hydrothermal performance of rectangular MCs with fish-scale-type fins. First, they conducted their work experimentally, and then they employed Ansys Fluent commercial software to calculate the PD, friction factor, Nu , and HT rate based on their obtained experimental data. The simulations were completed at three Re values: 250, 650, and 1050. The outcomes

showed that adding fish-scale-type fins could improve HT in the investigated MC.

Liu et al. [4] conducted experiments to calculate the HT rate and PD in the rectangular MCs. They employed longitudinal vortex generators (VGs) to improve the HT rate. The various numbers of paired VGs with various angles of attack were used in the tested MC with Re ranging from 170 to 2000. They proved that longitudinal VGs could enhance HT performance significantly.

Steinke and Kandlikar [5] considered single-phase liquid friction factors in MCs. They demonstrated that conventional Stokes and Poiseuille flow theories are applicable to single-phase liquid flow in MCs. They extensively examined the PD's components and offered new experimental data. The suggested method precisely determines the elements of the total PD, providing better agreement with the accepted theory.

Gonul et al. [6] surveyed the impacts of delta winglet-type VGs inside a MC. They used response surface methodology for the optimization of their VGs, or in other words, to improve HT. The MC's hydraulic and thermal performances were computed for some parameters, such as various angles of attack, VG arrangement, various distances between VGs, various lengths and heights of VGs, and various Re values. The VG height was indicated as the most effective factor among the geometric parameters.

Gonul and Okbaz [7] improved an MC's thermal performance with rectangular VGs. They used ANSYS Fluent 19.1 to compute three-dimensional turbulent flow and heat transfer in the MC. The response surface methodology was utilized for the optimization of VG parameters. The results showed that the maximum increase in heat transfer using VGs is approximately 230% whereas the increase in pressure loss is 950%.

Khan et al. [8] conducted a computational investigation of various turbulator arrangements in an MC heat sink. With Re values ranging from 200 to 800, the authors examined temperature, Nu , PD, and friction factor. They investigated five ways to set up the turbulators, with three MC widths and different heat flows from the wall. Their numerical simulation, in which they placed the turbulators on 75% of the MC length with a pitch of 0.75 mm, had the highest Nu at an Re of 800.

Vasilev et al. [9] made various models of MC heat sinks and tested them in the lab and with computers. They used circular pin fins inside the MC with two diameters and five Re values between 100 and 1000 at various heights. They studied PD, Nu , and thermal resistance of the MCs and obtained the optimal pin parameters. They demonstrated that Nu and PDs depended directly on fin height. They acquired the largest Nu and PD when the height reached its maximum value.

Tan et al. [10] ran a unique computer simulation of how the topology of MC heat sinks works. Initially, they designed ternate veiny, lateral veiny, snowflake-shaped, and spider-netted MCs. Then they utilized fluid-thermal coupling computational studies, and the findings indicated that the spider-netted one generated the greatest HT performance. Therefore, they selected and optimized the spider-netted one for the cooling system. Finally, they compared the HT rates of spider-netted and straight MCs. The practical outcomes show that its thermal performance was better than the other one's.

Soleymani et al. [11] examined the HT in a MC with pin-fins at the hotspot zone described in their study. They used Ansys Fluent, a commercial program, to study the effects of 143 heat sink pin-fins in the centers of 20 MCs. They conducted all simulations at Re ranging from 200 to 1000 and heat flux ranging from 300 to 900 W/cm². The outcomes illustrated that pin-fin shape, pin-fin angle, Re, and hotspot heat flux significantly affected HT, PD, and pumping power. They found that a rectangular pin-fin with rounded edges was better than other shapes.

Pan et al. [12] focused on the flow and HT performance of a cylindrical pin-fin manifold MC heat sink. They made multiple comparisons between the pin-fin manifold MC and the rectangular one and found that the HT performance of the pin-fin manifold MC was better at the same mass flux. On the other hand, in the same operating conditions, the PD of the pin-fin manifold MC was higher.

Mohammed et al. [13] worked on the influence of MC heat sink shapes on HT performance computationally. They studied various sizes and shapes of MCs, including zigzag, curvy, wavy, straight, and step ones. They presumed Re between 100 and 1000 with a constant heat flux of 100 W/m² from the top plate, and they identified temperature, HTC, PD, friction factor, and wall shear stress as the leading factors. The results indicated that the zigzag MC was the optimal one, considering the studied parameters.

Moosavi et al. [14] investigated a three-dimensional MC with a transverse VG and porous medium computationally. They solved single-phase laminar flow of the fluid domain following the finite-volume method, and the Re was thought to range from 125 to 1000 during simulations. They made findings regarding HT and PD as well as the number of transverse VGs at various heights. The findings illustrated that the use of VG and porous media caused a rise in the thermal performance ratio, indicating the normalization of the altered HTC and PD at low and high Re.

Khan et al. [15] conducted computer simulations with straight, wavy, and double-wavy MC heat sinks. They compared their models' HT performance in terms of three channel shapes with three alumina-based nanofluid concentrations. In their study, they used the commercial software Ansys Fluent to figure out what happened to an incompressible fluid when the Re increased from 100 to 900. The HT performance of the entire wavy channel was more than double that of the straight channels and increased as the Re increased. Owing to the creation of secondary vortices at the curved section, it has been discovered that wavy channels enhance convective HT compared to straight channels. Compared to the pure fluid flow in the channel situation, the dual wavy channels demonstrated the greatest enhancement, 8%, and the largest thermal performance factor, 2.2, when 6% nanoparticles were added to all channels.

Zhang et al. [16] numerically studied a three-dimensional model of a multi-core chip-microchannel heat sink. Based on constructal theory, they optimized the fin structure in the chip microchannel for non-uniform power partitioning utilizing a genetic algorithm to find the optimal structure. The results showed that the maximum temperature can be lowered by 6.75 K when the Re is 750 and the overall pressure loss can be lowered by 54.1% when Re is 750 when comparing the optimal fin arrangement with the dense pin-fin array [16].

Yang et al. [17] studied HT and flow behaviors in the backward-facing step MCs numerically. They applied various nanofluids with some volume fractions for cooling flow in these MCs. They found that the investigated nanofluids could absorb more heat from the surface and that the reattachment point depended on the Re. The Nu of the bottom surface increased with the increase in the Re and

step height. They concluded that HT performance depended on the volume fractions of nanofluid.

Yang et al. [18] considered water/alumina nanofluid in a rectangular MC numerically. They benefited from three techniques for increasing HT in the MC. They injected flow with and without nanofluid from six points to the MC at three Re values: 1, 10, and 100. The results showed that the first, second, and third techniques improved the Nu by up to 25, 3.5, and 28%, respectively. On the other hand, these techniques increased the PD in the MC, as well.

Ali et al. [19] denoted the HT of an MC with various fins numerically. They employed rectangular, twisted, and zig-zag fins inside the MC as well as Al₂O₃ nanofluid coolant with volumetric concentrations ranging from 0 to 3% in these simulations. The results showed that the maximum Nu was obtained for the case, including the combination of the zig-zag fin and 3% Al₂O₃ nanofluid. Moreover, they emphasized that they achieved a minimum PD with the simulated MC, including the twist fin inside.

The heat exchanger that Kucukakca, Meral, and Parlak [20] utilized was a crossflow MC design made of aluminum and sized according to standard dimensions. Plates in heat exchangers typically have dimensions of 50 mm by 50 mm by 3 mm and were constructed of two plates arranged in a cross-flow configuration. They created an adequate experimental facility to carry out studies involving the movement of fluids and heat. In addition, they used ANSYS to model the HT and fluid flow properties in MCs. They compared the findings of fluid dynamics and experiments with those from CFD. The investigation revealed that the results of the experimental HT data closely aligned with the results of the CFD simulation.

Gaikwad and Mohite [21] conducted computational and experimental research to investigate the thermo-hydraulic properties of a new MC heat sink that had flow-disrupting pins. Instead of the traditional method of using pin-fins that originate from the base of the MC, the researchers introduced cylindrical pins from the top cover into the rectangular MC. They first investigated the influence of pin diameter and then determined the optimal pin diameter. Subsequently, they compared the performance with that of a standard MC. The inclusion of pins caused a full disruption of the velocity distribution and an increase in the studied MC's capacity for heat transfer; however, it came at the expense of a larger pressure drop penalty. The overall enhancement factor that might be attained with this method is 1.24. In their study, they provided correlations indicating the influence of channel width-to-pin diameter ratio on Nu and friction factor.

Kayaci et al. [22] expressed the HT performance and fluid flow behaviors in smooth and micro-fin tubes numerically. They used water and nanofluids with TiO₂ particles as coolants with helix angles ranging from 0 to 18°. They applied an artificial neural network to choose the suitable properties of nanofluids. They used the best results from this method in numerical simulations. They obtained the findings of temperature, pressure, and velocity distributions and compared them with other numerical and experimental studies in open sources.

A review of the literature shows that there is no study on the selection of geometrical factors affecting the thermal and hydraulic performances with low Re studied in this work either experimentally or numerically. Pin-finned MCs as macro- (conventional) and microscales have received significant attention lately as a result of better thermal-hydraulic performance in comparison to plain MCs. The current study showed that circular pin-fins affect the MC's hydraulic and thermal performance. The goal of the numerical work was to determine how the distance between fins affects hydraulic and thermal performance in laminar flow at various Re values. We examined three fin spacing-to-fin diameter ratios ($l/d = 2, 4, \text{ and } 6$), which were the main geometrical parameters that changed in the simulated MCs when the Re varied from 50 to 150. The PD results indicated the hydraulic performance, and the average outlet temperature and average Nu pointed to thermal performance to study these geometrical parameters' effect. The results of this study can be a reference for future studies. They can be used to compare other methods and improve heat transfer methods using nanofluids in this Re range.

2. Numerical method

2.1. Governing equations

Considering water flow in a microchannel, three-dimensional, steady-state, incompressible Navier-Stokes equations are numerically solved to obtain the pressure, velocity, and temperature fields for laminar flow inside MCs with and without fins of rectangular cross-section using the commercial solver ANSYS Fluent. The conservation of mass, momentum, and energy equation can be obtained in order as follows:

$$\nabla \cdot \vec{u} = 0 \quad (1)$$

$$\rho(\vec{u} \cdot \nabla \vec{u}) = -\nabla p + \mu \nabla^2 \vec{u} \quad (2)$$

$$\rho c_p (\vec{u} \cdot \nabla \vec{T}) = k \nabla^2 \vec{T} \quad (3)$$

All equations are iteratively solved. Convective terms are discretized with a second-order upwind scheme. A second-order accurate interpolation scheme is employed to compute pressure at the control surface. Gradients are calculated using the least squares cell-based method, which assumes linear variation in the values of any transported quantity between two adjacent cells. The limit of the governing equations' criteria convergence was chosen as 10^{-6} . We calculated all conservation equations until the criteria for convergence reached their limits.

2.2. Details of the computational model

Fig. 1 shows the computational domain and boundary conditions, as well as a detailed view of how the fins are set up on the bottom

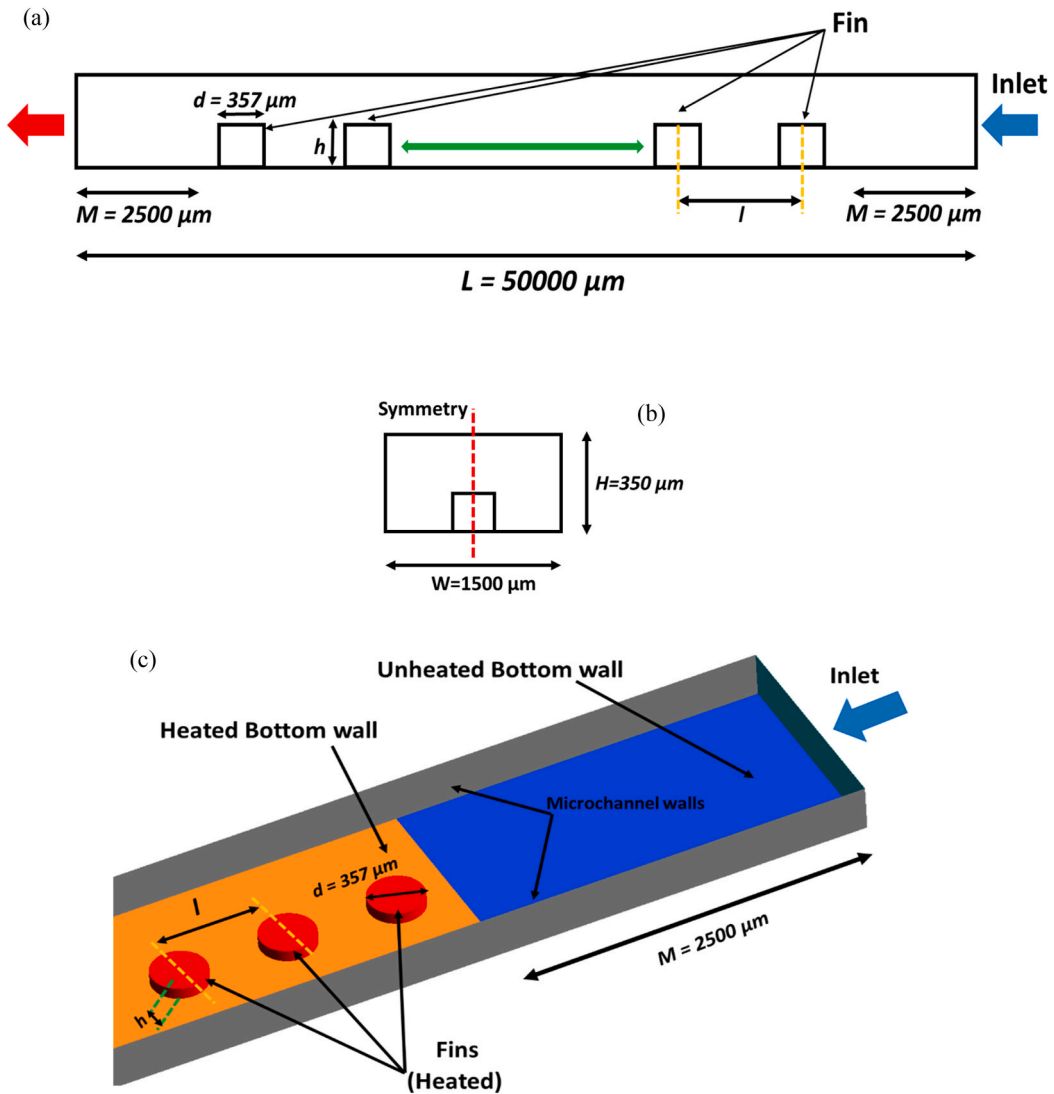


Fig. 1. Illustration of the solution domain and the boundary conditions with some relevant geometrical parameters: (a) side view, (b) front view, and (c) bottom wall configuration with fin-related geometrical parameters.

Table 1
The numerical simulations' parameters in the present study for MC with and without fins ($h/H = 0.25$).

Re	l/d	Case number
50	without fins	(case1)
75	without fins	(case2)
100	without fins	(case3)
125	without fins	(case4)
150	without fins	(case5)
50	2,4,6	(case 6), (case7), (case8)
75	2,4,6	(case 9), (case10), (case11)
100	2,4,6	(case12), (case13), (case14)
125	2,4,6	(case15), (case16), (case17)
150	2,4,6	(case18), (case19), (case20)

wall. The rectangular channel has a height of $350 \mu\text{m}$, width of $1500 \mu\text{m}$ width, and length of $50\,000 \mu\text{m}$, and the fins have a diameter of $375 \mu\text{m}$ and height of $87.5 \mu\text{m}$. The center-to-center distance between two successive fins is denoted with l . Given that the geometry and the flow field are symmetrical about the vertical longitudinal mid-plane, only the half-width of the channel is considered in the numerical calculations to save solution time; therefore, the symmetry condition is applied to one of the surfaces that coincide with the

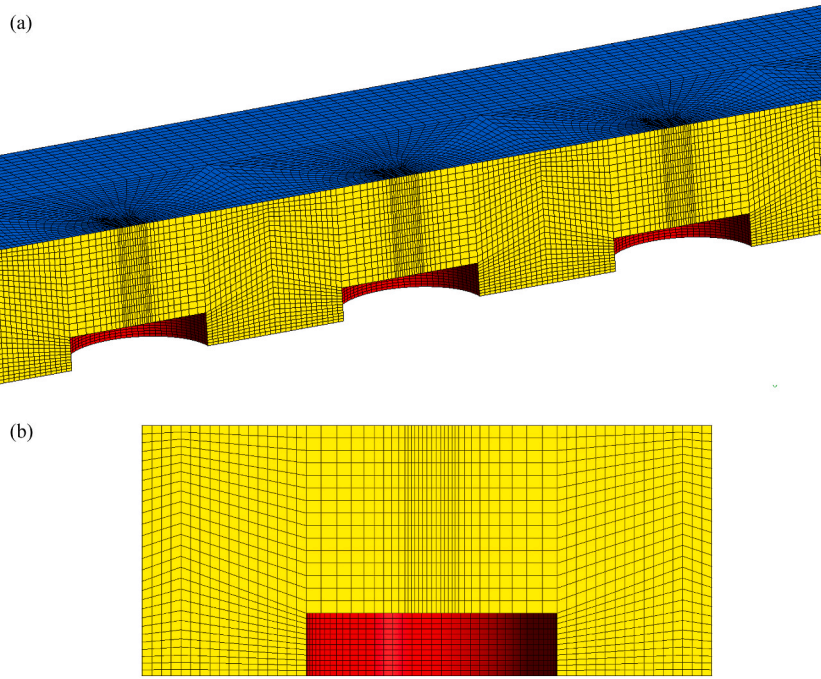


Fig. 2. (a) The numerical mesh used in the calculations and (b) an enlarged view around the fin surface.

Table 2
Results of the mesh independence study.

Number of elements	Nu	ϵ_{Nu} [%]
0.75×10^6	4.97	–
1.40×10^6	5.03	1.20
2.60×10^6	5.05	0.39

symmetry plane. The symmetry condition assumes zero normal gradients of the transport variables. The channel inlet is modeled by employing a velocity inlet boundary condition, where velocity and temperature have fixed values. Inlet velocity values are adjusted according to the corresponding Re , and the fluid temperature is $T_i = 300$ K for all cases. At the channel outlet, an outflow condition is assigned that allows for extrapolation from upstream neighboring cells, assuming zero streamwise gradients of flow variables. The remaining surfaces, which are the top, bottom, and side boundaries, as well as fin surfaces, are modeled as no-slip walls. The constant wall temperature of 323.15 K is applied at the bottom wall except for two short sections 2500 μm long adjacent to the inlet and outlet and fin surfaces. The remaining wall surfaces are treated as adiabatic, i.e., with zero heat flux. A total of 20 cases are simulated in the present study. Five of them include the investigations of HT in a MC without fins at various Re values. The presence of fins at various Re values has been studied in other cases. Table 1 presents the summary of the numerical runs.

For the simulations shown in Fig. 2, a structured mesh with prismatic elements is made. A mesh independence study is conducted to minimize the effect of grid quality, where the average Nu , Nu_m , is considered. Mesh configurations with approximately 0.75, 1.4, and 2.6 million elements are generated for the geometrical case 18 for $l/d = 2$ and $h/H = 0.25$, and the Re depending on the hydraulic diameter is 150. Accordingly, the sizing configuration of the mesh with 2.6 million elements is used in all the numerical calculations, with a deviation of less than 1% in Nu as shown in Table 2.

2.3. Data reduction

The Re is based on the hydraulic diameter of the MC and is calculated as follows:

$$Re_{Dh} = \frac{\rho U_{in} D_h}{\mu} \quad (4)$$

The local and average Nu (Nu_x and Nu) are calculated as follows:

$$Nu_x = \frac{q_w D_h}{(T_w - T_b)k} \quad (5)$$

Table 3
Comparison of the average Nu and the apparent friction factor.

	Nu	ϵ [%]	f_{app}	ϵ_{fapp} [%]
Experimental (Liu et al., 2011)	5.68	–	0.061	–
Numerical (present study)	5.75	1.23	0.057	–6.56

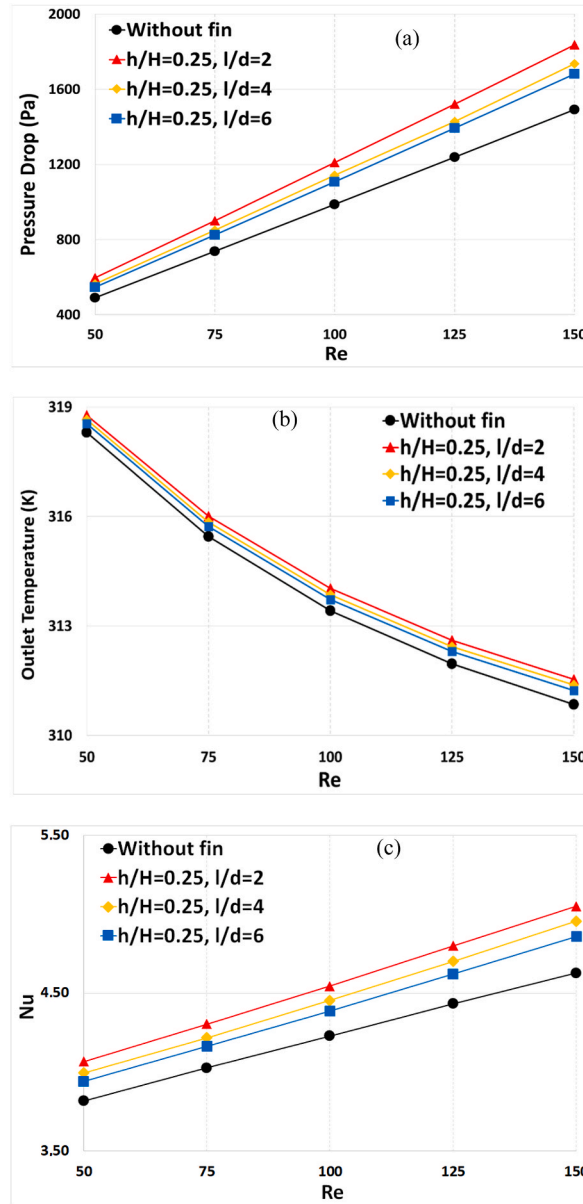


Fig. 3. (a) Variation of average PD, (b) variation of average outlet temperature, and (c) variation of average Nu with Re for MC with and without fins.

$$Nu = - \frac{D_h}{k} \ln \left(\frac{T_w - T_i}{T_w - T_o} \right) \frac{\dot{m} c_p}{A} \tag{6}$$

The Fanning friction factor, which is the form of the wall shear stress and doesn't depend on its size, is defined as

$$f = \tau_w / (0.5\rho U_{in}^2) \tag{7}$$

To consider the entrance effects, especially for developing flows, an apparent friction factor, f_{app} , based on the Fanning friction

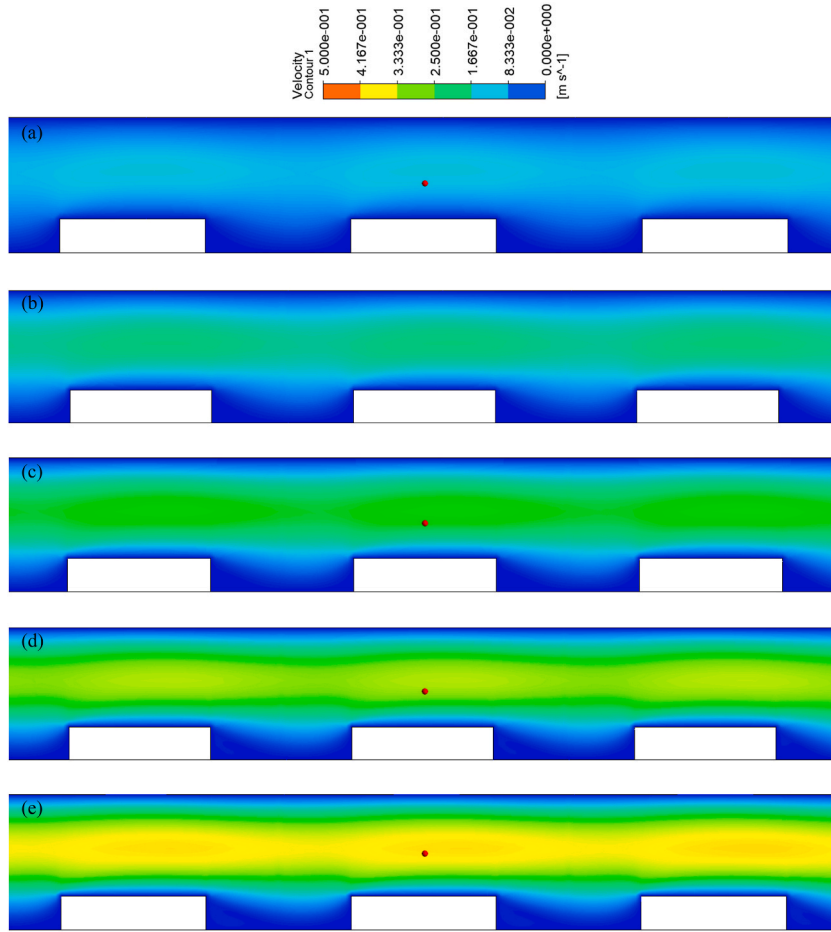


Fig. 4. Velocity distribution (m/s) contour plots at the symmetry plane along MC length for $l/d = 2$, for (a) $Re = 50$ (case 6), (b) $Re = 75$ (case 9), (c) $Re = 100$ (case 12), (d) $Re = 125$ (case 15), and (e) $Re = 150$ (case 18).

factor which is defined in terms of the PD along the channel is given in Eq. (8):

$$f_{app} = \frac{\Delta P}{2\rho U_{in}^2} \frac{D_h}{L} \quad (8)$$

It should be noted that in Eqs. (4)–(8), the properties of water are considered constant and independent of temperature.

2.4. Validation of the numerical model

For the validation of the numerical method employed in the present study; water flow in an MC of a rectangular cross-section without fins is numerically simulated, and the average Nu , and apparent friction factor, f_{app} , are compared to those obtained in the previous experimental study by Liu et al. [4], for $Re = 270$ (Table 3). Since Liu et al. [4] reported a significant dependence on temperature variation, second- and third-order polynomial correlations are introduced to the model temperature-dependent material properties of water for the numerical calculation presented in the existing work. Accordingly, a reasonably good agreement between the computational and practical outcomes for Nu and f_{app} is evident with an absolute error of less than 2 and 7%, respectively. Therefore, it is concluded that the numerical setup adopted herein can reliably be employed for further calculations.

3. Results and discussion

Hydraulic and thermal performances for various fin spacing arrangements were computed in this part. The results of PD, average outlet temperature, and Nu were obtained and compared with a smooth MC. The results from the numerical analyses are summarized in the following paragraphs.

Fig. 3a shows an increase in PD with Re in all MC models. The MC without fins (smooth channel) has the lowest PD compared to the MCs with fins at all Re values. Fin spacing (the distance between two fins) plays an important role in PD. Decreasing the distance between fins causes them to behave as obstacles and restrict flow in an MC. PD increases with reduced fin spacing. The results of PDs indicate the highest PDs are created at all MCs with the smallest fin spacing ($l/d = 2$) for all Re values (cases 6, 9, 12, 15, and 18). The

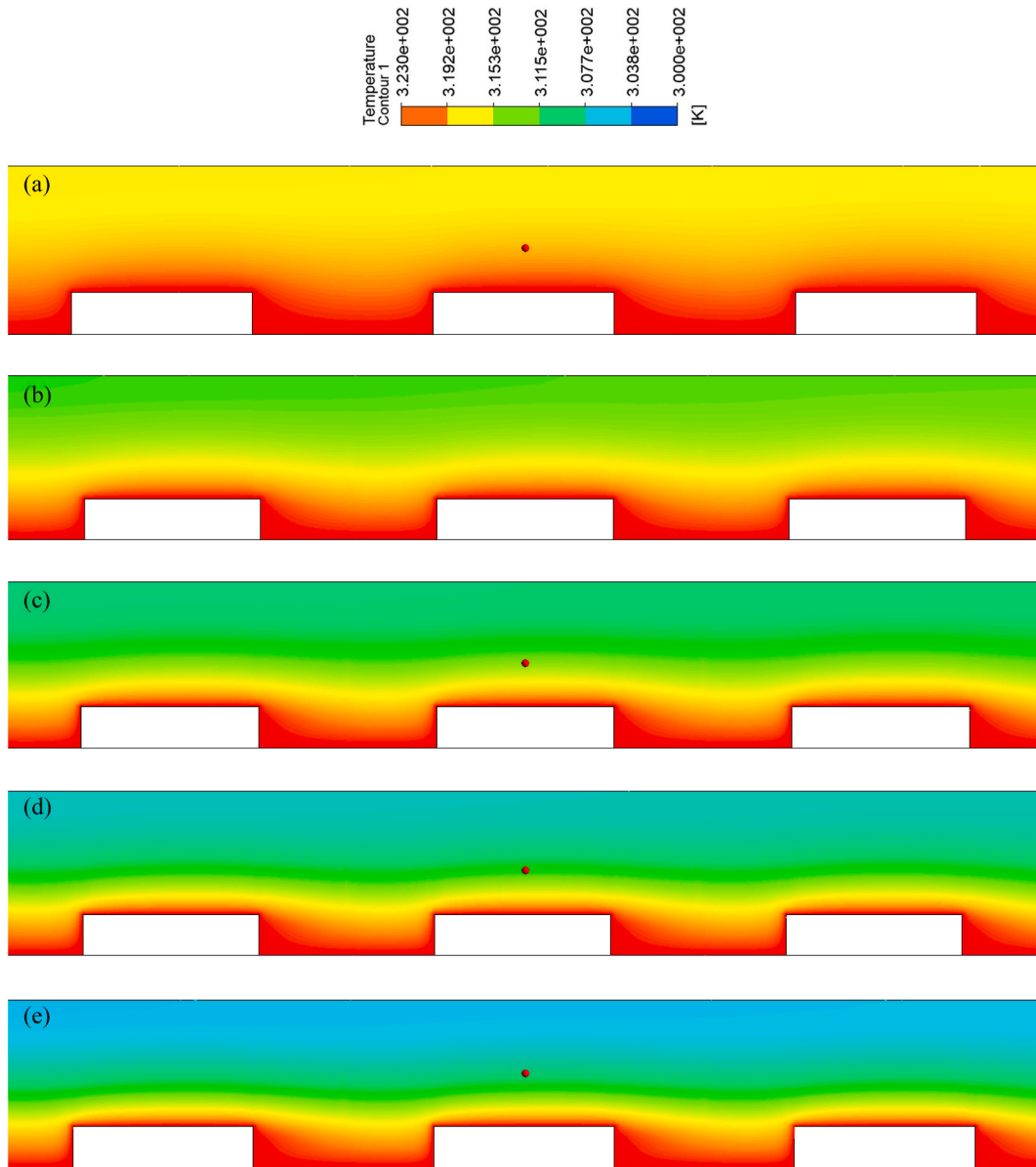


Fig. 5. Temperature distribution (K) contour plots at the symmetry plane along MC length for $l/d = 2$, for (a) $Re = 50$ (case 6), (b) $Re = 75$ (case 9), (c) $Re = 100$ (case 12), (d) $Re = 125$ (case 15), and (e) $Re = 150$ (case 18).

PD of the MC with fins (case 18) is nearly 23% higher than that of the MC without fins (case 5) at $Re = 150$. Additionally, PD increases by nearly 207% when the Re varies from 50 (case 6) to 150 (case 18) for the lowest fin spacing ($l/d = 2$). The PD of the smallest fin spacing ($l/d = 2$) is nearly 9% more than that of the highest one ($l/d = 6$), for Re ranging from 50 to 150. Fig. 3b illustrates a change in average outlet temperature as a function of the Re for all MCs. The average outlet temperature of the MC without fins is lower than that of MCs with fins. The average outlet temperature decreases with increasing Re for all MC models. It should be seen that the average outlet temperature rises with decreasing fin spacing for all Re values. On the other hand, the average outlet temperature of the MC with the lowest fin spacing ($l/d = 2$) is greater than those of the other ones ($l/d = 4$ and 6) for all Re . The average outlet temperature of the MC with fins (case 18) is improved by nearly 0.23% compared to the MC without fins (case 5) for $Re = 150$. In all MC models (cases 1, 6, 7, and 8), the cooling fluid's average outlet temperature increased by nearly 6.5% compared with the average inlet temperature when the Re was 50. In this manner, the cooling fluid heats up by nearly 4% at the outlet compared with the average inlet temperature when the Re is 150 (cases 5, 18, 19, and 20). Fig. 3c demonstrates that MCs with fins have a larger average Nu than the ones without fins. The MC with the smallest fin spacing ($l/d = 2$) has the largest average Nu compared with other MC models. The average Nu of the MC with fins (case 18) is nearly 9% higher than that of the MC without fins (case 5) when the Re is 150. Besides, the average Nu of the MC with fins (case 18) is nearly 4% more than the MC with fins (case 20) when the Re is 150. Similar to this trend, the average Nu of the

MC with fins (case 6) is nearly 6.5% higher than the MC without any fins (case 1) when the Re is 50. In addition, the Nu of the MC with fins (case 6) is nearly 3.3% higher than that of the MC with fins (case 8) when the Re is 50. It is also realized that the average Nu rises with increasing Re for all MC models. The average Nu increases by nearly 24% for the smallest fin spacing ($l/d = 2$) when the Re ranges from 50 to 150. Decreasing the distance between fins causes fluctuation in the flow area, and then the velocity increase is observed around the fins in the MCs; therefore, the HT and average Nu increase in the MC. Moreover, the average Nu of the MC without fin increases by nearly 21% when the Re ranges from 50 to 150.

Fig. 4 represents the velocity contour plots of the last three fins in the MC for the smallest fin spacing ($l/d = 2$) at an Re of 50 (case 6), 75 (case 9), 100 (case 12), 125 (case 15), and 150 (case 18). They are plotted from the symmetry plane of the MC. Velocity is found to be low between each fin. On the other hand, maximum velocity appears between the tip of the fins and the top side of the MC wall. It is also realized that the value of maximum velocity grows with increasing Re.

Fig. 5 illustrates the same operating conditions as Fig. 4. It clearly shows that the highest cooling fluid temperature appears around and between fins in all MC models. The cooling fluid's temperature decreases with increasing Re. It is realized that the temperature difference between the fin surface and the top side of the MC wall is small, at a Re of 50. However, at high Re, these determined temperature differences are higher than those with a smaller Re.

4. Conclusions

A rectangular MC with a circular pin-fin was considered in this study. Water as a cooling fluid was applied at Re values ranging from 50 to 150. The three-dimensional computational domain was calculated based on laminar flow. Inlet fluid temperature and bottom wall temperature were fixed at 300 and 323.15 K, respectively. The PD, average outlet temperature, and average Nu were numerically computed. This numerical study focused on the selection of geometrical factors affecting the thermal and hydraulic performances with low Re, which had never been studied experimentally or numerically. The results are summarized as shown below.

- The PD and average Nu increased with increasing Re for all MC models.
- The PD of the MC with the lowest l/d ($l/d = 2$) was greater than the other ones studied ($l/d = 4$ and 6).
- The PD of the MC with the lowest l/d ($l/d = 2$) was nearly 23 and 9% larger than those for the smooth one and the one with the largest fin spacing ($l/d = 6$), respectively.
- The average outlet temperature decreased with an increase in Re for all MC models.
- The maximum average temperature of cooling flow between the inlet and outlet was obtained at the lowest l/d ($l/d = 2$) when the Re was lowest (Re=50).
- The highest average Nu was obtained when l/d was 2 and Re was 150.
- The average Nu of the MC with the lowest l/d ($l/d = 2$) at the largest Re (Re=150) was nearly 9 and 4% greater than those for the smooth one and the one with the largest l/d ($l/d = 6$), respectively.

Author statement

Mahdi Tabatabaei Malazi: Methodology, Data curation, Writing- Original draft preparation **Kenan Kaya:** Methodology, Data curation, Writing- Original draft preparation **Ahmet Selim Dalkılıç:** Conceptualization, Reviewing and Editing.

Declaration of competing interest

The authors declare that they have no known competing financial interests or personal relationships that could have appeared to influence the work reported in this paper.

Data availability

Data will be made available on request.

Acknowledgment

All authors would like to express their appreciation for the financial support to Prof. Dr. Somchai Wongwises from King Mongkut's University of Technology Thonburi (KMUTT) in Thailand. The third author thanks KMUTT for the support during his visit to KMUTT.

References

- [1] P.S. Lee, S.V. Garimella, D. Liu, Investigation of heat transfer in rectangular microchannels, *Int. J. Heat Mass Tran.* 48 (2005) 1688–1704.
- [2] H. Lu, M. Xu, L. Gong, X. Duan, J.C. Chai, Effects of surface roughness in microchannel with passive heat transfer enhancement structures, *Int. J. Heat Mass Tran.* 148 (2020), 119070.
- [3] P. Dey, S.K. Saha, Fluid flow and heat transfer in microchannel with porous bio-inspired roughness, *Int. J. Therm. Sci.* 161 (2021), 106729.
- [4] C. Liu, J.T. Teng, J.C. Chu, Y.I. Chiu, S. Huang, S. Jin, T. Dang, R. Greif, H.H. Pan, Experimental investigations on liquid flow and heat transfer in rectangular microchannel with longitudinal vortex generators, *Int. J. Heat Mass Tran.* 54 (2011) 3069–3080.
- [5] M.E. Steinke, S.G. Kandlikar, Single-phase liquid friction factors in microchannels, *Int. J. Therm. Sci.* 45 (2006) 1073–1083.
- [6] A. Gonul, A. Okbaz, N. Kayaci, A.S. Dalkilic, Flow optimization in a microchannel with vortex generators using genetic algorithm, *Appl. Therm. Eng.* 201 (2022), 117738.
- [7] A. Gonul, A. Okbaz, Enhanced performance of a microchannel with rectangular vortex generators, *J. Therm. Eng.* 9 (2023) 260–278.

- [8] M. Khan, S.Z. Shuja, B.S. Yilbas, H. Al-Qahtani, A case study on innovative design and assessment of a microchannel heat sink with various turbulators arrangements, *Case Stud. Therm. Eng.* 31 (2022), 101816.
- [9] M.P. Vasilev, R. Sh Abiev, R. Kumar, Effect of circular pin-fins geometry and their arrangement on heat transfer performance for laminar flow in microchannel heat sink, *Int. J. Therm. Sci.* 170 (2021), 107177.
- [10] H. Tan, L. Wu, M. Wang, Z. Yang, P. Du, Heat transfer improvement in microchannel heat sink by topology design and optimization for high heat flux chip cooling, *Int. J. Heat Mass Tran.* 129 (2019) 681–689.
- [11] Z. Soleymani, M. Rahimi, M. Gorzin, Y. Pahamli, Performance analysis of hotspot using geometrical and operational parameters of a microchannel pin-fin hybrid heat sink, *Int. J. Heat Mass Tran.* 159 (2020), 120141.
- [12] Y. Pan, R. Zhao, Y. Nian, W. Cheng, Study on the flow and heat transfer characteristics of pin-fin manifold microchannel heat sink, *Int. J. Heat Mass Tran.* 183 (2022), 122052.
- [13] H.A. Mohammed, P. Gunnasegaran, N.H. Shuaib, Influence of channel shape on the thermal and hydraulic performance of microchannel heat sink, *Int. Commun. Heat Mass Tran.* 38 (2011) 474–480.
- [14] R. Moosavi, M. Banihashemi, C.X. Lin, P.Y.A. Chuang, Combined effects of a microchannel with porous media and transverse vortex generators (TVG) on convective heat transfer performance, *Int. J. Therm. Sci.* 166 (2021), 106961.
- [15] M.Z.U. Khan, M.Y. Younis, N. Akram, B. Akbar, U.A. Rajput, R.A. Bhutta, E. Uddin, M.A. Jamil, F.P.G. Marquez, F.B. Zahid, Investigation of heat transfer in wavy and dual wavy micro-channel heat sink using alumina nanoparticles, *Case Stud. Therm. Eng.* 28 (2021), 101515.
- [16] J. Zhang, W. Guo, Z. Xie, X. Guan, X. Qu, Y. Ge, Optimization of fin layout in liquid-cooled microchannels for multi-core chips 41 (2023), 102615.
- [17] D. Yang, B. Sun, T. Xu, B. Liu, H. Li, Experimental and numerical study on the flow and heat transfer characteristic of nanofluid in the recirculation zone of backward-facing step microchannels, *Appl. Therm. Eng.* 199 (2021), 117527.
- [18] L. Yang, K. Du, Numerical simulation of nanofluid flow and heat transfer in a microchannel: the effect of changing the injection layout arrangement, *Int. J. Mech. Sci.* 172 (2020), 105415.
- [19] A.M. Ali, M. Angelino, A. Rona, Numerical analysis on the thermal performance of microchannel heat sinks with Al₂O₃ nanofluid and various fins, *Appl. Therm. Eng.* 198 (2021), 117458.
- [20] Z. Küçükakça Meral, N. Parlak, Experimental research and CFD simulation of cross flow microchannel heat exchanger, *J. Therm. Eng.* 7 (2021) 270–283.
- [21] V.P. Gaikwad, S.S. Mohite, Performance analysis of microchannel heat sink with flow disrupting pins, *J. Therm. Eng.* 8 (2022) 402–425.
- [22] N. Kayaci, M. Balçilar, M. Tabatabaei Malazi, A. Celen, O. Yıldız, A.S. Dalkilic, S. Wongwises, Determination of the single-phase forced convection heat transfer characteristics of TiO₂ nanofluids flowing in smooth and micro-fin tubes by means of CFD and ANN analyses, *Curr. Nanosci.* 9 (2013) 61–80.